

A robotic learning and generalization framework for curved surface based on modified DMP

Xianfa Xue^a, Jiale Dong^a, Zhenyu Lu^b, Ning Wang^{b,*}

^a Key Laboratory of Autonomous Systems and Networked Control, School of Automation Science and Engineering, South China University of Technology, Guangzhou, China

^b Bristol Robotics Laboratory, University of the West of England, Frenchay, Coldharbour Ln, BS16 1QY, UK



ARTICLE INFO

Article history:

Available online 29 November 2022

Keywords:

Continuous drag demonstration
Modified DMP
Curve drawing experiments
Learning and generalization framework

ABSTRACT

How to reproduce and generalize the skills acquired by demonstrating is a hot topic for researchers. (1) A compliant continuous drag demonstration system based on discrete admittance model was designed to continuously and smoothly drag or demonstrate. (2) The modified DMP including the scaling factor and the force coupling term was used to improve the poor generalization ability of the classical DMP. (3) Curve drawing experiments were carried out to show the effectiveness of our proposed learning and generalization framework.

© 2022 The Authors. Published by Elsevier B.V. This is an open access article under the CC BY license (<http://creativecommons.org/licenses/by/4.0/>).

1. Introduction

Humans can adapt well to posture and strength when performing tasks in unknown environments. However, robots need to employ a complex set of planning algorithms for specific tasks [1–3]. To enable robots to learn human manipulation skills, learning by demonstration (LfD) has been studied in recent years [4,5]. In the absence of kinematic models, trajectory planning and assembly problems can be well solved using LfD. Human demonstration is when a human expert teaches a robot how to perform certain specialized skills. The motion trajectory will be recorded and used to train the skill model [6]. Robotic manipulators not only repeat learned skills, but are often expected to generalize to new tasks and situations. This requires skill models that are easy to train and adapt to new tasks and environments. For LfD, one of the difficulties and challenges is generalization, which requires learning skills to deal with uncertain and unknown tasks [7]. Numerous methods have been proposed, optimization-based trajectory planning methods [8], data-driven methods [9,10], to handle trajectory generation in the above-mentioned situations [11,12].

Most industrial robots only open the position servo interface instead of the torque control interface, and do not provide the interface to obtain the dynamic parameters of robots. This means that using the drag demonstration based on robotic dynamic compensation needs to identify the dynamic parameters and friction model [13]. However, there are often large errors in the identification process, which will affect the performance of drag

demonstration [14]. Although most industrial robots, such as UR robots, have their own drag demonstration function, it is difficult to drag the manipulator to follow a smooth and continuous spatial trajectory. In many cases, they can only obtain a continuous and smooth trajectory through interpolation after single point teaching, which makes the demonstrating process time-consuming and laborious. Therefore, it is of great practical value to develop a continuous and compliant demonstration scheme for industrial robots [15].

Dynamical motion primitive (DMP) is widely used in trajectory planning of robotic arms to imitate the behavior of human tutor [16–18]. The DMP model is essentially a second-order nonlinear system (spring–damping system) to approximate a motion trajectory. DMP and its evolutionary structure have been proposed by many researchers, and motion information is represented by a set of nonlinear differential equations. They are widely used in imitation learning and trajectory generalization [19,20]. In order to solve the problems that the original DMP could not produce the right trajectories under some special cases, some researchers improved DMP model. Some researchers combined neural network control with DMP to solve complex tasks with special constraints, such as obstacle avoidance and interaction with the external environment [21–23], most of which added coupling terms based on the basic transformation system [24–26].

In this paper, the reference trajectory on the flat surface is obtained by continuously drag demonstration, and then the in-situ reproduction, flat and curved surface generalization are carried out by the modified DMP model. The contributions can be summarized as follows. (1) A continuous drag teaching algorithm based on discrete admittance model is designed, which improves the problem that it is difficult for Elite industrial robot to teach by dragging compliantly and effortlessly. (2) The classical DMP

* Corresponding author.

E-mail address: Katie.Wang@brl.ac.uk (N. Wang).

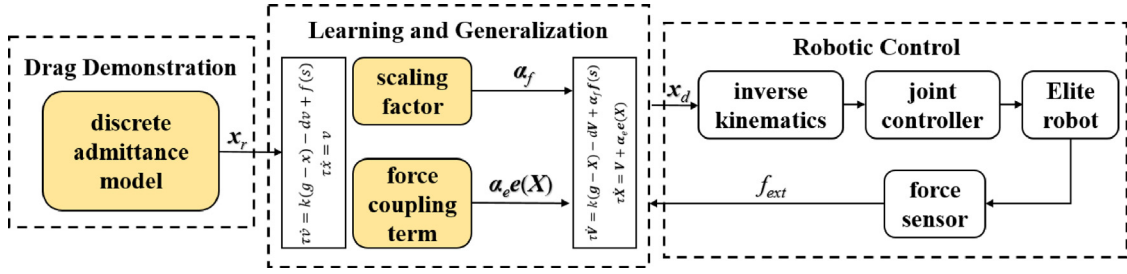


Fig. 1. Overview of the proposed robotic learning and generalization framework.

model is modified by introducing scaling factor and force coupling term, which improves the generalization ability of DMP model in flat and curved surface.

The rest of the article structure is organized as follows. In Section 2, materials and methods were described. Discrete admittance model, original DMP and modified DMP used in this paper are introduced. In Section 3, the experimental study is presented and then the effectiveness of the framework proposed in this paper is verified via Elite robot. Finally, in Section 4, conclusions were given to summarize the whole paper.

2. Materials and methods

2.1. Overview of the framework

The overall structure block diagram of the proposed learning and generalization framework is shown in Fig. 1. First, reference trajectories are obtained by using the method of LfD. In this part, we propose a continuous drag demonstration method based on discrete admittance model to improve the problem that some industrial robots cannot drag compliantly and effortlessly. Then the classical DMP model is improved by adding scaling factor and force coupling term. After that, through the learning, reproducing and generalizing of the modified DMP model, a new desired trajectory x_d is obtained. Finally, the validity of the proposed framework is verified by Elite robot.

2.2. Continuous drag demonstration based on discrete admittance model

The Elite robot used in this paper has poor continuity for drag demonstration, so the smooth dragging effect cannot be achieved only by adjusting the internal parameters such as starting force coefficient and friction coefficient. Therefore, we uses the open position servo interface of Elite robot to design the continuous drag demonstration based on the admittance controller.

The six-dimensional force acting on the drag tool is obtained from the six-dimensional force/torque sensor, and the obtained force data needs to be compensated to eliminate the influence of tool weight, sensor drift and installation inclination [27]. The specific force compensation method is the same as our previous research work paper [28]. The compensated six dimensional force data is then input into the designed discrete admittance model to calculate the expected speed and position of the current robot end. The specific calculation formula is:

$$\ddot{x}_r(k) = M_r^{-1}(k) [F_{ext}(k) - D_r(k) \dot{x}_r(k-1) - K_r(k)(x_r(k-1) - x_0)] \quad (1)$$

$$\dot{x}_r(k) = \ddot{x}_r(k) T_k + \dot{x}_r(k-1) \quad (2)$$

$$x_r(k) = \dot{x}_r(k) T_k + x_r(k-1) \quad (3)$$

where, x_0 indicates the initial desired position of the robot end, $\ddot{x}_r(k)$, $\dot{x}_r(k)$ and $x_r(k)$ are the expected acceleration, speed and

position of the current robot end calculated by the discrete admittance controller, $F_{ext}(k)$ represents the six dimensional force acting on the dragging tool. T_k is the control cycle, k represents the current time step. $M_r(k)$, $D_r(k)$ and $K_r(k)$ represent the inertia coefficient, stiffness coefficient and damping coefficient matrix of the discrete admittance controller respectively.

2.3. Original and modified dynamic movement primitives

The original DMP is usually used to represent motor skills and used to encode motion trajectories. DMP is essentially a second-order spring-damping system, which can be divided into discrete and rhythmic types. In this work, we focus on the former. The DMPs model can be expressed by the following formula [29]:

$$\tau \dot{v} = k(g - x) - dv + f(s) \quad (4)$$

$$\tau \dot{x} = v \quad (5)$$

$$\tau \dot{s} = -\alpha_1 s \quad (6)$$

where Eq. (4) represents a transformation system consisting of a second-order spring-damping system and a nonlinear function, x and v represent the position and velocity of the motion, respectively, k and d represent the spring constant and damping coefficient of the system, respectively, which are artificially designed parameters, usually let $k = d^2/4$, g denotes the target position of the motion, τ denotes the time scaling constant, s is the phase of the system, determined by Eq. (6). It decays from the initial value 1 to 0 with time, then model will become a stable second-order spring-damping system. α_1 is a positive constant, $f(s)$ is a nonlinear function, which is defined as follows:

$$f(s) = \frac{\sum_{i=1}^N \psi_i \cdot \omega_i}{\sum_{i=1}^N \psi_i} \cdot (g - x_0) s \quad (7)$$

$$\psi_i = \exp(-h_i(x - c_i)^2) \quad (8)$$

where c_i and h_i are the center and width of the i th Gaussian function respectively, x_0 is the initial position, N is the number of Gaussian functions, and ω_i is the weight of the i th Gaussian function.

The original DMP model can translate and scale the demonstration trajectory. Nevertheless, for the transformation on the spatial curved surface, the original model learns the nonlinearity in three directions separately, which will lead to the shape distortion of the spatial curve. In order to fully describe the position and posture of the manipulator, 6 DMPs are employed to denote positions and X-Y-Z Euler angles. Therefore, we modified the classical DMP model as follows:

$$\tau \dot{V} = k(g - X) - dV + \alpha_f^{(T)} f(s) \quad (9)$$

$$\tau \dot{X} = V + \alpha_e e(X) \quad (10)$$

$$\tau \dot{s} = -\alpha_1 s \quad (11)$$

where $\alpha_f^{(T)} = \text{diag}([\alpha_{f_x}, \alpha_{f_y}, \alpha_{f_z}, \alpha_{f_\alpha}, \alpha_{f_\beta}, \alpha_{f_\gamma}])$ is the transformation factor between the surface to be generalized and the

robot coordinate system, and $\{T\}$ is the transformation matrix. $\mathbf{e}(\mathbf{X})$ is the output error of admittance model, that is, the deviation between the current position and the reference position of admittance model. α_e is adjustment constant matrix. $\mathbf{X} = [x, y, z, \alpha, \beta, \gamma]^T$ and $\mathbf{V} = [v_x, v_y, v_z, \omega_\alpha, \omega_\beta, \omega_\gamma]^T$ are state variables of the system. In this paper, we use a supervised learning method called locally weighted regression algorithm (LWR) to determine the model parameters ω [30].

2.4. Stability and convergence of the modified DMP

The stability and convergence of the modified DMP are proved [31]. The modified DMP can be written as the following equation:

$$\begin{aligned} \tau^2 \ddot{x} &= k \left(g + \frac{\alpha_f f + \tau \alpha_e \dot{e}(x) + d \alpha_e e(x)}{k} - x \right) - d \tau \dot{x} \\ &= k(u - x) - d \tau \dot{x} \end{aligned} \quad (12)$$

where u is a time-variant input to the linear spring-damper system. Then the Laplace transform is performed on (12):

$$G(s) = \frac{x(s)}{u(s)} = \frac{k}{\tau^2 s^2 + d \tau s + k} \quad (13)$$

On the basis of Routh criterion, the condition for the bound input bound output (BIBO) stability of a second-order system is $k > 0$ and $d > 0$. When time t approaches infinity, $\alpha_e e(x)$ reaches 0. And the variable s approaches 0, the function f disappears and no longer works. The transformation system of the modified DMP develops into a linear second-order system. The state variable x converges to g with time t to infinity.

3. Experiment and analysis

In this section, the improved continuous drag demonstration method based on admittance model was tested by a 6-DOF Elite-EC66 robot as shown in Fig. 2, and the generalization performance of the improved DMP and the original DMP in the flat and curved surface will be compared respectively. The ATI Mini45 Force/Torque sensor was mounted on the end of the manipulator through the connecting flange to sense the interacting force between the end-effector and the environment in real time. The pen fixing tool made by 3D printing was used to fix the marking pen and was also used as a handle during drag demonstration. A clamping position was designed at the end of the pen fixing tool, and the marking pens of different colors were stably fixed through the coupling device. The force sensor and the upper computer communicated by the UDP protocol, whose sampling rate and control rate were 100 Hz and 50 Hz, respectively.

3.1. Continuous drag demonstration

In order to verify the effectiveness of the improved drag demonstration method, we implemented the following comparative experiments. Before the drag teaching, a standard sine curve was given on the experimental plane as the reference trajectory, as shown by the red curve in Fig. 3(a). At first, the proposed drag method was used. The program was run in the remote mode of Elite robot. The discrete admittance model parameters were set as follows: $M_r = \text{diag}[0.5, 0.5, 0.5, 0.5, 0.5, 0.5]$; $D_r = \text{diag}[0.1, 0.1, 0.8, 10, 10, 10]$; $K_r = \text{diag}[0.02, 0.02, 0.02, 0.9, 0.9, 0.9]$. Then the operator held the black handle of the pen fixing tool and performed drag teaching along the reference track, as shown by the black curve in Fig. 3(d). At the second step, the self-contained drag teaching function of Elite robot was used as a contrast. In the Elite teaching mode, the built-in parameters were set as follows: the forward and reverse friction coefficients of each shaft were 5%, and the starting coefficient were 10%. The operator

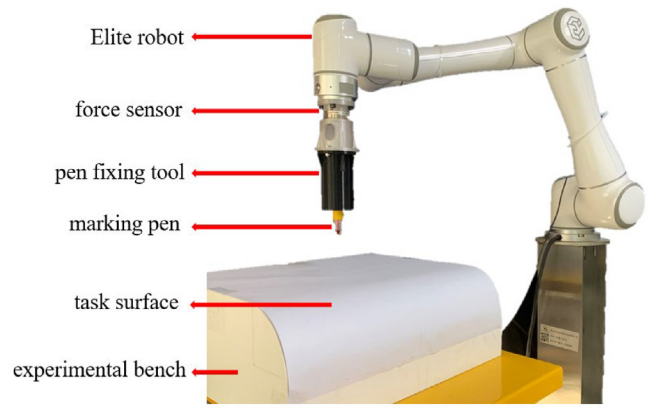


Fig. 2. Experimental platform based on Elite robot.

pressed the teaching button at the end of the manipulator to drag teaching, as shown by the blue curve in Fig. 3(f). During the demonstration process, trajectory coordinates under the two drag methods were recorded respectively, and the spatial curve was shown in Fig. 4.

Combining Figs. 3 and 4, it can be clearly seen that our drag demonstration method based on the discrete admittance model has a good performance. Even if the built-in parameters such as friction coefficient are adjusted to the most compliant state, there are still problems such as jamming and overshooting under the drag teaching function of Elite. So those problems may bring a lot of burden to human tutor and make it difficult to follow the reference trajectory accurately. Our method, on the other hand, can follow the target curve compliantly, coherently, and accurately.

3.2. Drawing task on different surface

In this section, the effectiveness of our modified DMP algorithm was verified. We performed the reproduction and generalization of the demonstration trajectory on flat and curved surfaces, respectively. In order to better reflect the advantages of our algorithm, the original DMP algorithm was also used for comparative experiments.

3.2.1. Reproducing and generalizing on flat surface

We still used the sine curve as our teaching reference trajectory. The pose information data of the reference trajectory were input into the modified DMP and the original DMP model for training. The parameters were set as: $d = 20$, $k = 20^2/4$, $\tau = 0.5$, $N = 80$. First, the trajectory was reproduced between the start point and the end point of the reference trajectory, that is, the two DMP models were reproduced without changing the start point $(-551.030, 131.399, -17.560)$ and end point $(-660.021, 130.034, -17.538)$. The effect was shown in Figs. 5 and 6. As was seen from the trajectory curves, two methods were both able to basically complete the reproduction of the given reference trajectory. From the details, the peak position of the original DMP reproduced trajectory in the Y direction presented an amplitude attenuation of 2 mm. Instead, the modified DMP can basically keep the original amplitude of the demonstration curve. We used the wave height to characterize the amplitude of the curve, that is, the vertical distance between the peak point and the trough point. The wave heights of the three curves were shown in Table 1.

In another set of experiments, we changed the start point and end point, in which case we verified the generalization ability of the DMP model for translating and scaling. The new start and end

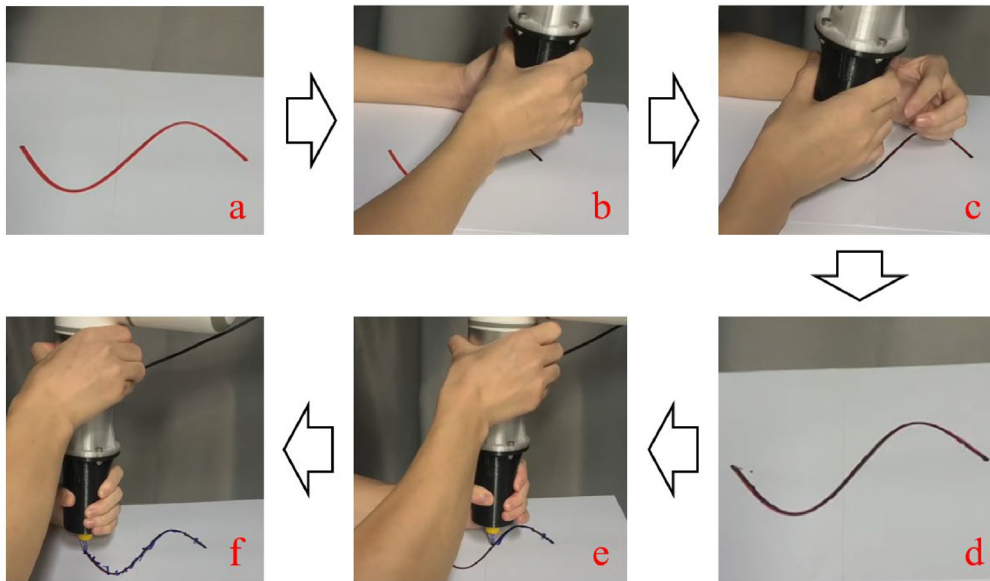


Fig. 3. Comparative experiment process between continuous demonstration based on discrete admittance model and built-in drag demonstration of Elite robot.

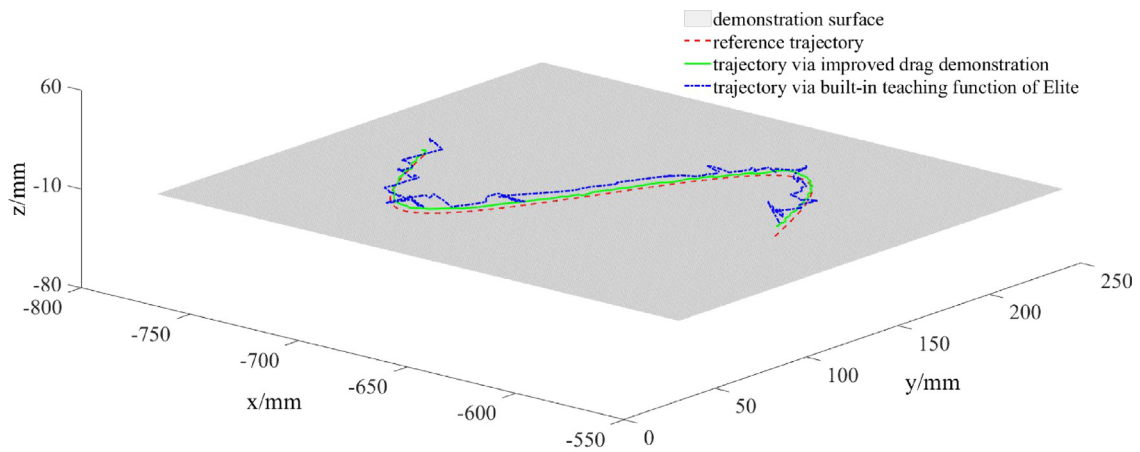


Fig. 4. Spatial curves of different demonstration methods.

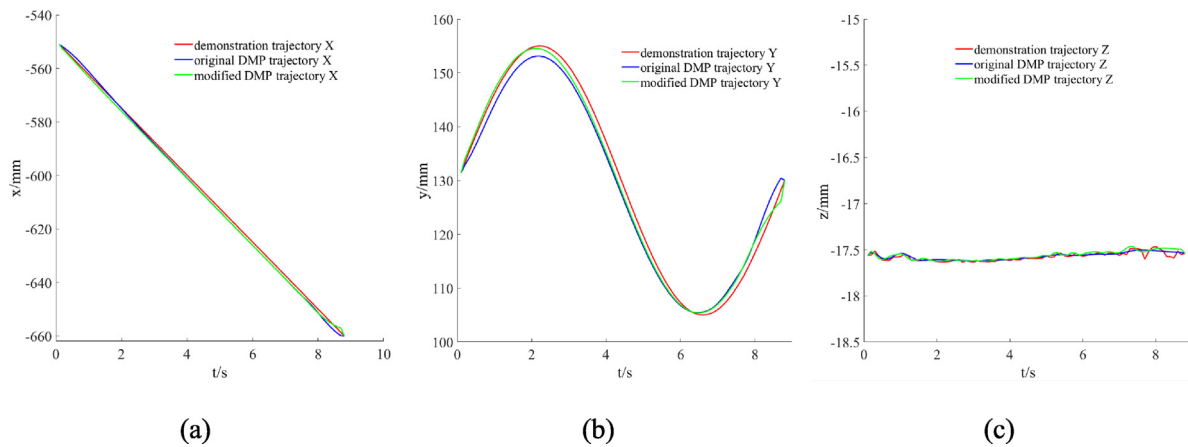


Fig. 5. Reproducing trajectory in X, Y and Z direction at the original start and end point. (a) Reproducing trajectory in X direction. (b) Reproducing trajectory in Y direction. (c) Reproducing trajectory in Z direction.

coordinates are $(-701.698, 132.420, -17.538)$ and $(-807.597, 129.739, -17.518)$. The trajectory curves after generalization via the two methods are shown in Figs. 7 and 8. As was seen from

the trajectory curves, two methods were both able to basically complete the generalization of the given reference trajectory on the flat surface. However, for the original DMP, the amplitude

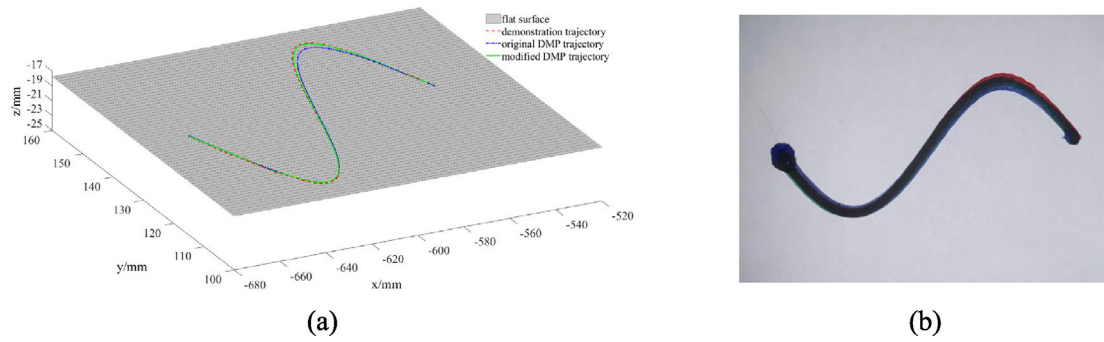


Fig. 6. Spatial curves reproduced on the flat surface and its actual experimental effect. (a) Spatial curves reproduced on the flat surface. (b) Actual experimental effect via Elite robot.

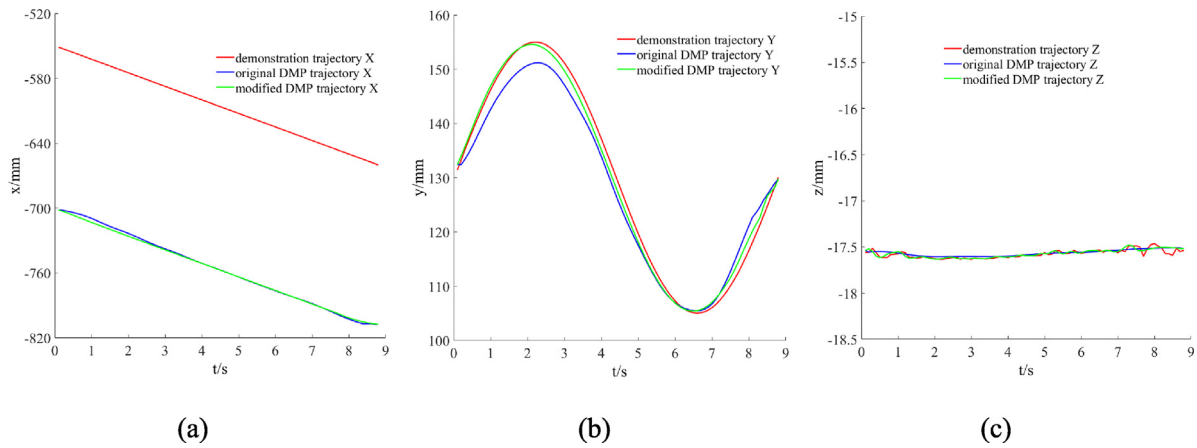


Fig. 7. Generalizing trajectory in X, Y and Z direction at the new start and end point. (a) Generalizing trajectory in X direction. (b) Generalizing trajectory in Y direction. (c) Generalizing trajectory in Z direction.

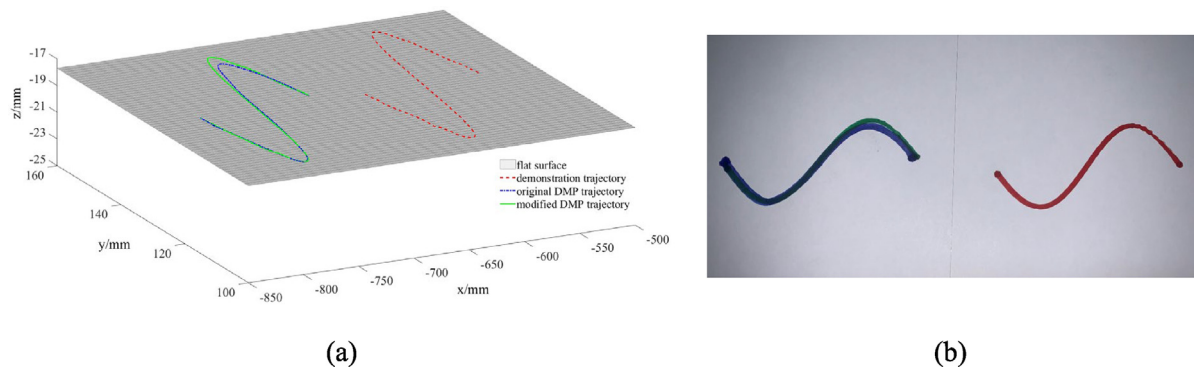


Fig. 8. Spatial curves generalized on the flat surface and its actual experimental effect. (a) Spatial curves generalized on the flat surface. (b) Actual experimental effect via Elite robot.

Table 1
Wave heights of three curves during reproduction.

Trajectory	Demonstration	Original DMP	Modified DMP
Wave height (mm)	49.979	47.669	49.161

attenuation in the Y direction at the peak of the curve still existed and increased to 4 mm. For the modified DMP algorithm, the original amplitude was still kept almost unchanged. The wave heights of the three curves during generalization were shown in Table 2.

In general, the above two groups of reproduction and generalization experiments showed that the two DMPs were both

Table 2
Wave heights of three curves during generalization.

Trajectory	Demonstration	Original DMP	Modified DMP
Wave height (mm)	49.979	45.725	49.158

able to realize the trajectory reproduction and simple generalization on the flat surface. However, the modified DMP algorithm showed better performance in terms of maintaining the shape and amplitude of the demonstration trajectory.

3.2.2. Generalizations on curved surface

In this part, we tested the generalization ability of the modified DMP model on the curved surface. We also used the flat

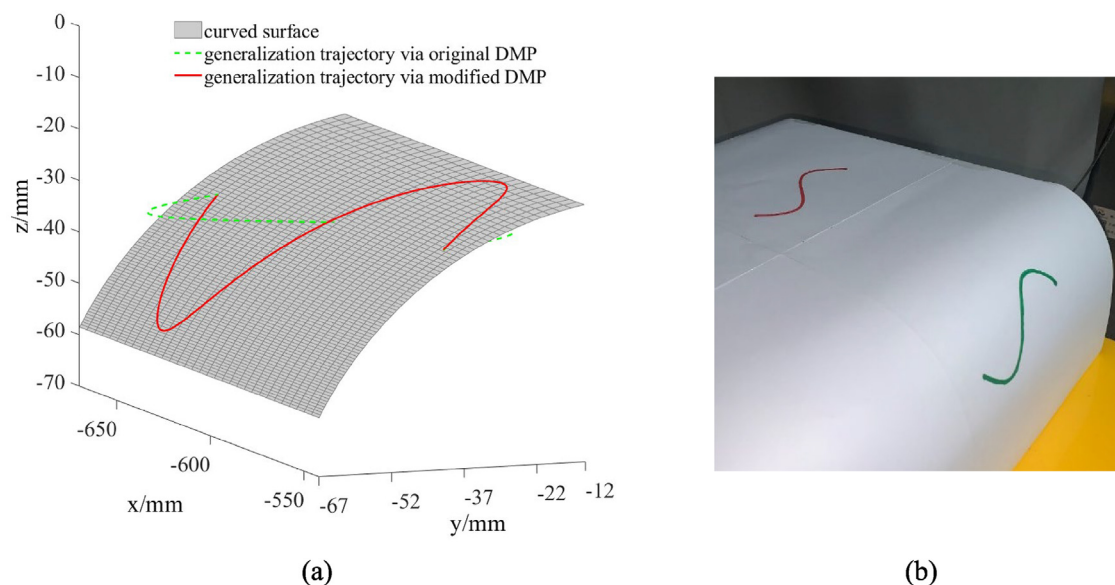


Fig. 9. Spatial curves generalized on the curved surface and its actual task effect. (a) Spatial curves generalized on the curved surface. (b) Actual task effect via Elite robot.

surface teaching trace of the previous two groups of experiments as the reference trajectory, and then generalized it to the side curved surface of the experimental bench. The three-dimensional size information of the test bench model used was known. The new start and end coordinates on the curved surface were $(-551.698, -37.580, -28.765)$ and $(-657.597, -43.254, -32.265)$, respectively. The spatial trajectory curves after generalization via the two DMP models were shown in Fig. 9(a), and the actual task effect was shown in Fig. 9(b).

Fig. 9(a) showed that the modified DMP were able to realize curved surface generalization. The generalized trajectory was still similar to the sinusoidal curve and accurately fit on the target curved surface. However, when inputting a new start point and end point on the given curved surface into the original DMP, it still generalized according to the plane where the Z coordinate was located, and failed to fit the target curved surface, as shown by the green curve in Fig. 9(a). The surface drawing task was a failure at last. At the same time, as was shown from the actual task effect Fig. 9(b) that the modified DMP algorithm successfully completed the curved surface generalization task.

4. Conclusions

In this paper, a robotic learning and generalization framework for curved surface was proposed. Based on the discrete admittance model, a compliant continuous drag demonstration scheme was designed, and the comparison experiment was carried out with the built-in teaching function of Elite robot. It can help the instructor overcome the instability and resistance in the teaching process, so as to reduce the burden of the instructor and improve the stability of the demonstration operation. In addition, the classical DMP model was modified to improve the generalization performance, then the experimental test was completed through the curve drawing task. Though this study did not focus on the precise force control, in future work, we will consider the design of the force controller and apply this framework to surface engraving tasks.

Declaration of competing interest

The authors declare that they have no known competing financial interests or personal relationships that could have appeared to influence the work reported in this paper.

Data availability

The detailed parameters of used model and controller are given in the manuscript. The results are computed on the Matlab 2018a software, while the relevant results are also given in the manuscript.

Acknowledgments

This work was supported in part by the National Natural Science Foundation of China (NSFC) under Grant 61803039, in part by Industrial Key Technologies R & D Program of Foshan, China under Grant 2020001006308.

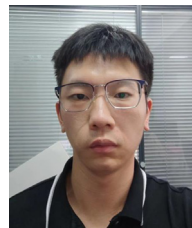
References

- [1] C. Zeng, Y. Li, J. Guo, Z. Huang, N. Wang, C. Yang, A unified parametric representation for robotic compliant skills with adaptation of impedance and force, *IEEE/ASME Trans. Mechatronics* 27 (2) (2021) 623–633.
- [2] P. Pastor, L. Righetti, M. Kalakrishnan, S. Schaal, Online movement adaptation based on previous sensor experiences, in: *IEEE/RSJ International Conference on Intelligent Robots & Systems*, 2011, <http://dx.doi.org/10.1109/IROS.2011.6095059>.
- [3] H. Huang, C. Yang, C. Chen, Optimal robot-environment interaction under broad fuzzy neural adaptive control, *IEEE Trans. Cybern.* 51 (7) (2021) 3824–3835.
- [4] D. Papageorgiou, Z. Doulgeri, Learning by demonstration for constrained tasks, in: *2020 29th IEEE International Conference on Robot and Human Interactive Communication (RO-MAN)*, 2020.
- [5] C. Zeng, S. Li, Z. Chen, C. Yang, F. Sun, J. Zhang, Multifingered robot hand compliant manipulation based on vision-based demonstration and adaptive force control, *IEEE Trans. Neural Netw. Learn. Syst.* (2022) <http://dx.doi.org/10.1109/TNNLS.2022.3184258>.
- [6] N. Wang, C. Chen, C. Yang, A robot learning framework based on adaptive admittance control and generalizable motion modeling with neural network controller, *Neurocomputing* 390 (2019) 260–267, <http://dx.doi.org/10.1016/j.neucom.2019.04.100>.
- [7] H. Ravichandar, A.S. Polydoros, S. Chernova, A. Billard, Recent advances in robot learning from demonstration, *Annu. Rev. Control Robot. Auton. Syst.* 3 (2020) 297–330, <http://dx.doi.org/10.1146/annurev-control-100819-063206>.
- [8] M. Vochten, W. Decre, E. Aertbelien, J.D. Schutter, Shape-preserving and reactive adaptation of robot end-effector trajectories, *IEEE Robot. Autom. Lett.* 6 (2) (2021) 667–674, <http://dx.doi.org/10.1109/LRA.2020.3048674>.
- [9] D. Kappler, F. Meier, J. Issac, J. Mainprice, C.G. Cifuentes, M. Wuthrich, V. Berenz, S. Schaal, N. Ratliff, J. Bohg, Real-time perception meets reactive motion generation, in: *International Conference on Robotics and Automation*, Vol. 3, (3) 2018, pp. 1864–1871.

- [10] C. Zeng, X. Chen, N. Wang, C. Yang, Learning compliant robotic movements based on biomimetic motor adaptation, *Robot. Auton. Syst.* 135 (2021) <http://dx.doi.org/10.1016/j.robot.2020.103668>.
- [11] S. Qiu, W. Guo, D. Caldwell, F. Chen, Exoskeleton online learning and estimation of human walking intention based on dynamical movement primitives, *IEEE Trans. Cogn. Develop. Syst.* 13 (1) (2021) 67–79.
- [12] Deng Mingdi, Kang Zhijun, C.L. Philip, Xiaoli Chen, Chu, A learning-based hierarchical control scheme for an exoskeleton robot in human-robot cooperative manipulation, *IEEE Trans. Cybern.* 50 (1) (2020) 112–125.
- [13] X. Li, H. Cheng, X. Liang, Adaptive motion planning framework by learning from demonstration, *Ind. Robot* 46 (4) (2019) 541–552.
- [14] C.L. Mueller, B. Hayes, Safe and robust robot learning from demonstration through conceptual constraints, in: *HRI '20: ACM/IEEE International Conference on Human-Robot Interaction*, 2020, pp. 588–590.
- [15] W. Meeussen, J. Rutgeerts, K. Gadeyne, H. Bruyninckx, J.D. Schutter, Contact-state segmentation using particle filters for programming by human demonstration in compliant-motion tasks, *IEEE Trans. Robot.* 23 (2) (2007) 218–231.
- [16] M. Lin, Z. Lu, S. Wang, R. Wang, The arm planning with dynamic movement primitive for humanoid service robot, in: *2020 5th International Conference on Advanced Robotics and Mechatronics (ICARM)*, 2020, pp. 513–518.
- [17] X. Ding, C. Fang, A novel method of motion planning for an anthropomorphic arm based on movement primitives, *IEEE/ASME Trans. Mechatron.* 18 (2) (2013) 624–636.
- [18] C. Zeng, S. Li, B. Fang, Z. Chen, J. Zhang, Generalization of robot force-relevant skills through adapting compliant profiles, *IEEE Robot. Autom. Lett.* 7 (2) (2021) 1055–1062.
- [19] A. Ijspeert, J. Nakanishi, S. Schaal, Movement imitation with nonlinear dynamical systems in humanoid robots, in: *Proceedings 2002 IEEE International Conference on Robotics and Automation*, 2002, pp. 1398–1403.
- [20] Y. Liang, W. Li, Y. Wang, R. Xiong, Y. Mao, J. Zhang, Dynamic movement primitive based motion retargeting for dual-arm sign language motions, in: *IEEE International Conference on Robotics and Automation (ICRA)*, 2020, pp. 8195–8201.
- [21] È. Pairet, P. Ardón, M. Mistry, Y. Petillot, Learning generalizable coupling terms for obstacle avoidance via low-dimensional geometric descriptors, *IEEE Robot. Autom. Lett.* 4 (4) (2019) 3979–3986.
- [22] H. Hoffmann, P. Pastor, D.H. Park, S. Schaal, Biologically-inspired dynamical systems for movement generation: Automatic real-time goal adaptation and obstacle avoidance, in: *Robotics and Automation*, 2009. *ICRA '09. IEEE International Conference on*, 2009, pp. 2587–2592.
- [23] C. Yang, C. Chen, C. Wei, W. He, R. Cui, Z. Li, Robot learning system based on adaptive neural control and dynamic movement primitives, *IEEE Trans. Neural Netw. Learn. Syst.* 30 (3) (2019) 777–787.
- [24] Z. Lu, N. Wang, C. Yang, A constrained DMPs framework for robot skills learning and generalization from human demonstrations, *IEEE/ASME Trans. Mechatronics* 26 (6) (2021) 3265–3275.
- [25] A. Gams, B. Nemec, A.J. Ijspeert, A. Ude, Coupling movement primitives: interaction with the environment and bimanual tasks, *IEEE Trans. Robot.* 30 (4) (2014) 816–830.
- [26] Z. Lu, N. Wang, C. Yang, A novel iterative identification based on the optimised topology for common state monitoring in wireless sensor networks, *Internat. J. Systems Sci.* 53 (1) (2022) 25–39.
- [27] L.J. Zhang, R.Q. Hu, W.M. Yi, Research on force sensing for the end-load of industrial robot based on a 6-axis force/torque sensor, *Acta Automat. Sinica* 43 (3) (2017) 439–447.
- [28] X. Xue, H. Huang, L. Zuo, N. Wang, A compliant force control scheme for industrial robot interactive operation, *Front. Neurorobot* 16 (2022) <http://dx.doi.org/10.3389/fnbot.2022.865187>.
- [29] A.J. Ijspeert, J. Nakanishi, S. Schaal, Learning rhythmic movements by demonstration using nonlinear oscillators, in: *IEEE/RSJ International Conference on Intelligent Robots & Systems*, 2002, pp. 958–963.
- [30] C.G. Atkeson, Using locally weighted regression for robot learning, in: *Proceedings IEEE International Conference on Robotics & Automation*, Vol. 2, 1991, pp. 958–963.
- [31] L. Han, P. Kang, Y. Chen, W. Xu, B. Li, Trajectory optimization and force control with modified dynamic movement primitives under curved surface constraints*, in: *2019 IEEE International Conference on Robotics and Biomimetics (ROBIO)*, 2019, pp. 1065–1070.



Xianfa Xue received the M.S. degree from Northwest A&F University, Shaanxi, China. He is currently pursuing the Ph.D. degree in South China University of Technology, Guangdong, China and majoring in electronics and information. His research interests include robotic learning from demonstration, intelligent control strategies and human-robot interaction.



Jiale Dong is currently studying for a master's degree at South China University of Technology, Guangdong, China, majoring in control science and engineering. His main research directions are robot teaching, human-computer interaction and intelligent learning strategies.



Zhenyu Lu received the Ph.D. degree in Northwestern Polytechnical University, Xi'an, China in 2019. He is currently working as a senior research fellow and a Marie Curie research fellow in Bristol Robotic Laboratory & University of the West of England, Bristol. He has published over 40 journals and conference papers about robotic teleoperation and control and robot skill learning. His research interests include teleoperation, human-robotics interaction and intelligent control.



Ning Wang is a Senior Lecturer in Robotics at the Bristol Robotics Laboratory, University of the West of England, United Kingdom. She received the M.Phil. and Ph.D. degrees in electronics engineering from the Department of Electronics Engineering, The Chinese University of Hong Kong, Hong Kong, in 2007 and 2011, respectively. Ning has rich project experience, she has been key member of EU FP7 Project ROBOT-ERA, EU Regional Development Funded Project ASTUTE 2020 and industrial projects with UK companies. She has been awarded several awards including best paper award of ICIRA'15, best student paper award nomination of ISCSLP'10, and award of merit of 2008 IEEE Signal Processing Postgraduate Forum, etc. Her research interests lie in signal processing, intelligent data analysis, human-robot interaction and autonomous driving.